Supplementary Data

Supplementary Figures

Figure S1

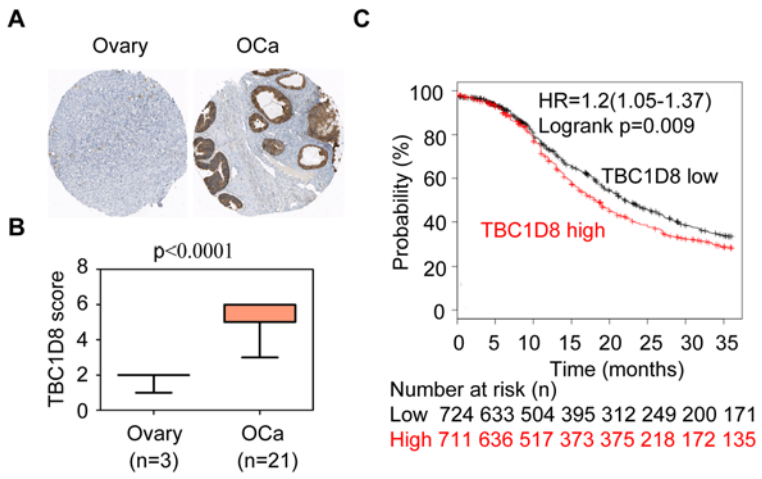

Figure S1. TBC1D8 is up-regulated in OVCA and the OVCA patients with high TBC1D8 level have shorter survival time. (A) Representative immunohistochemical (IHC) images of TBC1D8 in OVCA and normal ovarian tissues deposited in the Human Protein Atlas database. (B) The differences in TBC1D8 expression scores between OVCA and normal ovarian tissues are presented as a box plot from data deposited in The Human Protein Atlas database. (C) The Kaplan-Meier survival probability of OVCA patients according to TBC1D8 level from data deposited in The Human Protein Atlas database.

Figure S2

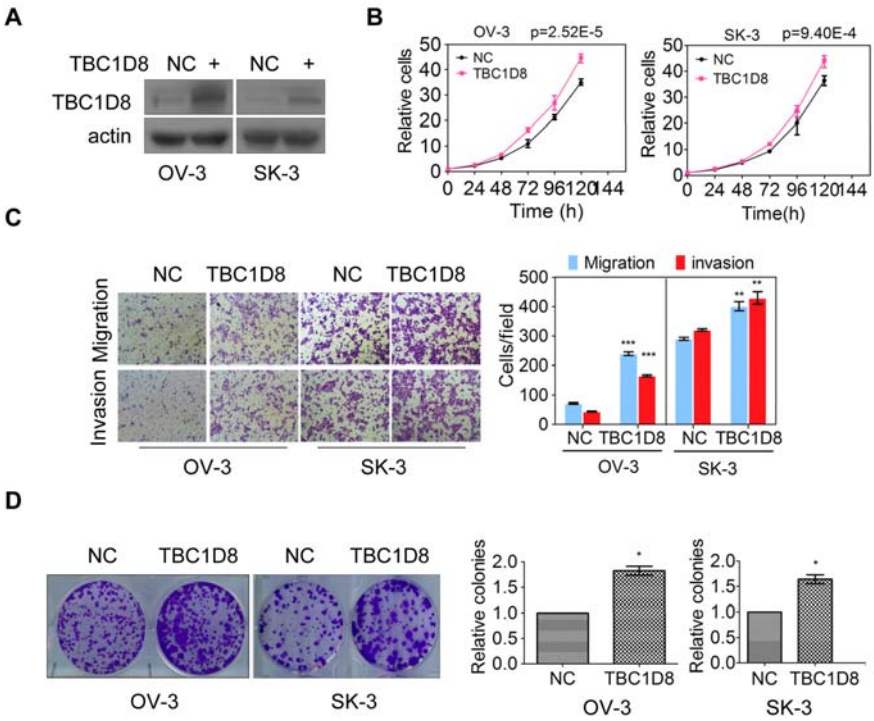

Figure S2. *TBC1D8* overexpression promotes a more malignant OVCA cell phenotype. (A, B) OV-3 and SK-3 cells were transfected with *TBC1D8* plasmid; the TBC1D8 protein level was detected by Western blotting (A); and the cell number was measured (B) (n=3). (C) OV-3 and SK-3 cells were transfected with *TBC1D8* plasmids, and the migration and invasion abilities were determined using transwell assays (left panel). The migrated and invasive cells were counted (right panel) (n=3). (D) OV-3 and SK-3 cells were transfected with *TBC1D8* plasmids, and the colony-forming abilities were measured after two weeks (left panel). The colony number was counted (right panel) (n=3).

Figure S3

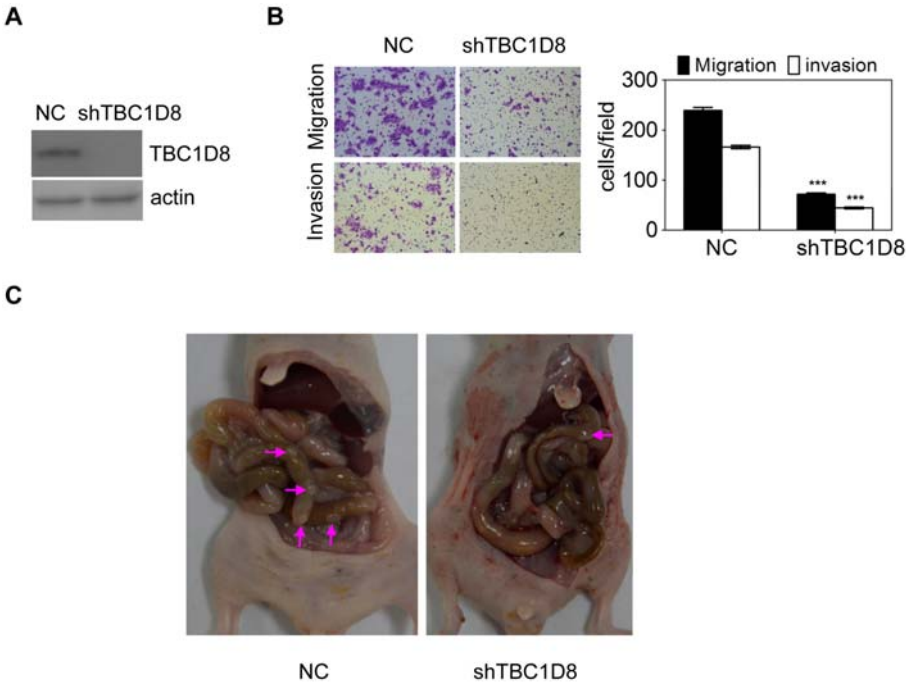

Figure S3. OV-3^{high} cells with *TBC1D8* expression stably silenced exhibited reduced migration and invasion abilities. (A) *TBC1D8* expression was silenced in OV-3^{high} cells with *TBC1D8* expression stably silenced. (B) The migration and invasion abilities were determined in OV-3^{high} cells with *TBC1D8* expression stably silenced. (C) The metastases to the mesentery, omentum, diaphragm and perihepatic sites in Figure 3F were observed.

Figure S4

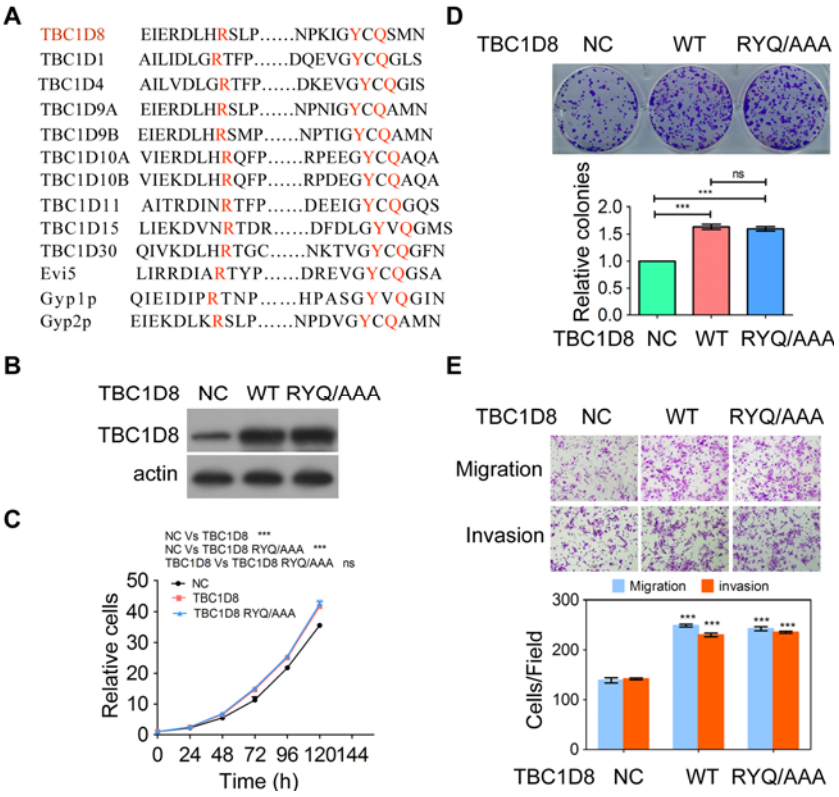

Figure S4. TBC1D8 promotes OVCA cell growth, colony formation, migration and invasion in a GAP activity-independent manner. (A) Alignment of the indicated regions of the GAP TBC domain in the TBC domain protein family. (B-E) The WT TBC1D8 or its RYQ/AAA mutant was transfected into OVCAR-3 cells, the indicated proteins (B), cell growth (C), colony formation (D), migration and invasion (E) were determined.

Figure S5

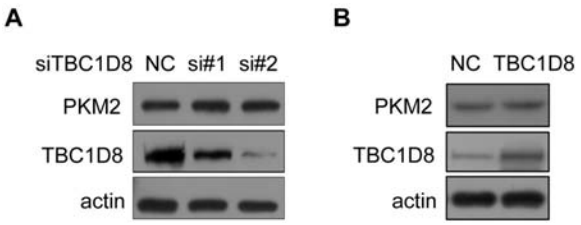

Figure S5. *TBC1D8* does not change the PKM2 protein level. OV-3^{high} and OV-3 cells were transfected with two anti-*TBC1D8* siRNAs (A) and *TBC1D8* plasmids (B) for 48 h, respectively, and the levels of the indicated proteins were determined by Western blotting.

Figure S6

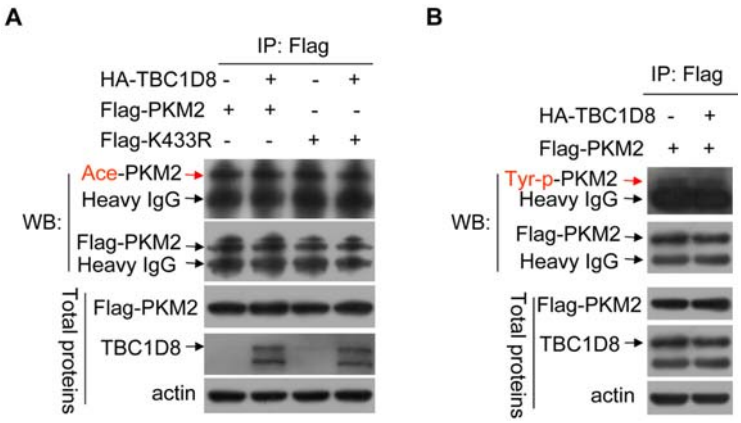

Figure S6. *TBC1D8* does not change the acetylation and phosphorylation levels of PKM2. (A) HEK293T cells were co-transfected with *TBC1D8* vectors together with wild-type or K433R mutant *Flag-PKM2* plasmids; Flag-PKM2 was IPed by anti-Flag antibody; and the PKM2 acetylation level was determined by Western blotting using an anti-acetylated lysine antibody. (B) HEK293T cells were co-transfected with *TBC1D8* vectors together with *Flag-PKM2* plasmids; Flag-PKM2 was IPed by an anti-Flag antibody; and the tyrosine-phosphorylation level of PKM2 was determined by Western blotting using an anti-phosphotyrosine antibody.

Figure S7

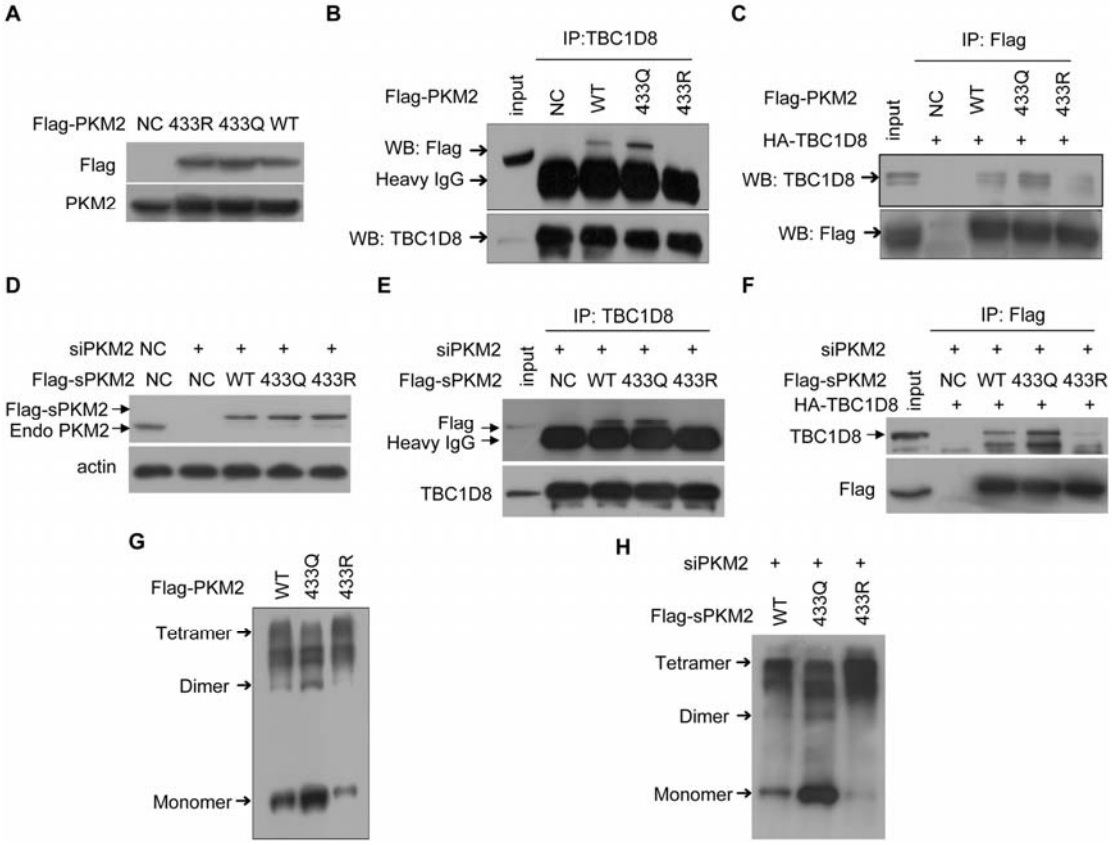

Figure S7. TBC1D8 interacts with dimeric PKM2, not tetrameric PKM2. (A) The indicated *Flag-PKM2* mutants were transfected into HEK293T cells, and the Flag-PKM2 protein level was detected. (B) The TBC1D8 complexes in OVCAR-3 cells, which were transfected with the indicated Flag-PKM2 vectors, were co-IPed using an anti-TBC1D8 antibody, and Flag-PKM2 expression in the complexes was detected using an anti-Flag antibody. (C) HEK293T cells were co-transfected with the indicated Flag-PKM2 mutants together with *HA-TBC1D8* vectors; the Flag-PKM2 complexes were co-IPed using an anti-Flag antibody; and HA-TBC1D8 expression in the complexes was detected using anti-HA antibody. (D) HEK293T cells were co-transfected with anti-PKM2 siRNAs together with the indicated synonymous mutant Flag-sPKM2 plasmids, the PKM2 levels were determined. (E) OVCAR-3 cells were co-transfected with anti-PKM2 siRNAs together with the indicated synonymous

mutant Flag-sPKM2 plasmids, the TBC1D8 complexes were co-IPed using an anti-TBC1D8 antibody, and Flag-PKM2 expression in the complexes was detected using an anti-Flag antibody. (F) HEK293T cells were co-transfected with anti-PKM2 siRNAs together with the indicated synonymous mutant Flag-sPKM2 plasmids and HA-TBC1D8 vector, the Flag-PKM2 complexes were co-IPed using an anti-Flag antibody; and HA-TBC1D8 expression in the complexes was detected using anti-HA antibody. (G) Cell lysates were prepared from HEK293T cells transfected with the indicated *Flag-PKM2* mutants, followed by cross-linking treatment. Flag-PKM2 was detected by Western blotting using an anti-Flag antibody. (H) Cell lysates were prepared from HEK293T cells transfected with anti-PKM2 siRNAs together with the indicated synonymous mutant Flag-sPKM2 plasmids, followed by cross-linking treatment. Flag-PKM2 was detected by Western blotting using an anti-Flag antibody.

Figure S8

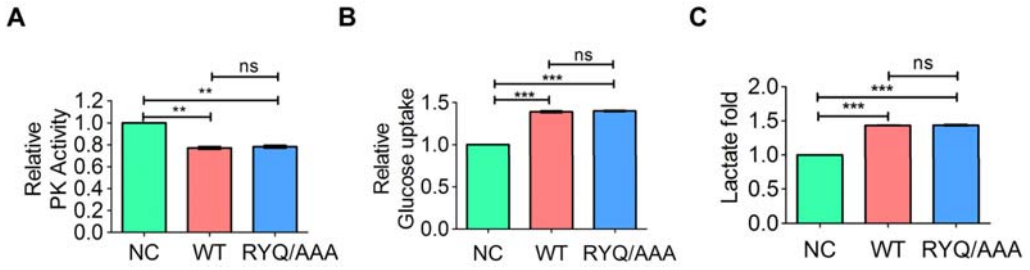

Figure S8. TBC1D8 inhibits PK activity and promotes aerobic glycolysis in a GAP activity-independent manner. The WT TBC1D8 or its RYQ/AAA mutant was transfected into OVCAR-3 cells, PK activity (A), glucose uptake (B), and lactate production (C) were determined (n=3).

Supplementary Tables

Supplementary Table S2. Correlations between TBC1D8 level and clinico-pathological features in 141 OVCA cases.

clinical characters	All cases	TBC1D8		*p* value*
		Low	High	
Age(Years)				0.078
＜50	65	14	51	
≥50	75	8	67	
Histological Grade				0.131
G1-G2	23	5	18	
G3	93	8	85	
Recurrence				0.003
Yes	111	12	99	
No	30	10	20	
pT status				0.048
1	45	11	34	
2-3	96	11	85	
pN status				0.045
0	111	21	90	
1	30	1	29	
pM status				0.197
0	120	21	99	
1	21	1	20	
Clinical Stage				0.048
Ⅰ-Ⅱ	45	11	34	
Ⅲ-Ⅳ	96	11	85	

*Pearson Chi-square test.

Supplementary Table S3. Univariate and multivariate analysis of different prognostic parameters in 141 patients with OVCA.

Clinical character	OS(months)			
	Univariate analysis		Multivariatie analysis	
	HR(95% CI)	p value*	HR(95% CI)	p value*
Age(≥50y vs.＜50y)	1.47(0.90-2.39)	0.119	1.17(0.70-1.95)	0.549
Histological Grade （G3 vs. G1-G2）	1.71(0.85-3.47)	0.134	0.88(0.41-1.91)	0.754
Recurrence of cacer(yes vs. no)	35.00(3.82-321.01)	0.002	282388.73 (0-3.74E+200)	0.956
pN status(1 vs. 0)	5.57(3.40-9.12)	0.000	1.24(1.01-4.20)	0.524
pM status(1 vs. 0)	6.29(3.65-10.84)	0.000	2.06(1.01-4.20)	0.046
pT status(2-3 vs.1)	11.24(4.09-30.91)	0.000	3.57(1.01-12.59)	0.047
TBC1D8	2.79(2.17-3.58)	0.000	2.11(1.61-2.78)	0.000

*Cox proportional hazard model.

Supplementary Table S5. Quantitative real-time PCR primers and the siRNA sequences used in this study.

Primers name		**Sequence (5'-3')**
MYC	Forward	GGAGGCTATTCTGCCCATTTG
	Reverse	CGAGGTCATAGTTCCTGTTGGTG
LDH	Forward	CATGGCCTGTGCCATCAGTATC
	Reverse	TGCCAGAGACAATCTTTGGTGTTC
GLUT1	Forward	TGTGGGCATGTGCTTCCAGTA
	Reverse	CGGCCTTTAGTCTCAGGAACTTTG
cyclinD1	Forward	GTGCATCTACACCGACAACTCC
	Reverse	GTTCCACTTGAGCTTGTTCACC
PDK1	Forward	GCTGTATGGCCTGCAAGATGA
	Reverse	AACATTCTGGCTGGTGACAGGA
GAPDH	Forward	GAAGGTGAAGGTCGGAGTC
	Reverse	AAGATGGTGATGGGATTTC
MEK5	Forward	ACAGCAGCCCAGCAGTCTCA
	Reverse	GTCCCGATATCGTATGTCTTGTTCA
siRNAs		**Sequence (5'-3')**
siTBC1D8#1	Sense	CCGAAUCACCACGCAGAAUTT
	Anti-sense	AUUCUGCGUGGUGAUUCGGTT
siTBC1D8#1	Sense	GCUUCACUCGUGUUUCAUUTT
	Anti-sense	AAUGAAACACGAGUGAAGCTT
NC siRNAs	Sense	GCACAAGCUGGAGUACAACUACATT
	Anti-sense	UGUAGUUGUACUCCAGCUUGUGCTT
siPKM2	Sense	GCCAUCUACCACUUGCAAUTT
	Anti-sense	AUUGCAAGUGGUAGAUGGCTT